Development of *Bristle Blasting* Process for Corrosion Removal and Generating Anchor Profile

Robert J. Stango, Ph.D., P.E.
Professor of Mechanical Engineering
and
Piyush Khullar
Research Assistant

Mechanical Engineering Department
1515 West Wisconsin Avenue
Marquette University
Milwaukee, WI 53233 USA

ABSTRACT

This technical paper introduces a newly developed surface preparation process termed *bristle blasting*, which utilizes a specially designed rotary power tool for simultaneously removing corrosion and generating an anchor profile. The process derives its name from sharp, hardened bristle tips which, upon striking the corroded surface, immediately retract, thereby creating a micro-indentation that both removes corrosion and simultaneously exposes fresh subsurface material. Consequently, the repeated collision/retraction of bristle tips with the corroded surface leads to a surface cleanliness and anchor profile that resembles surface prepared by grit blasting processes.

Performance of the bristle blasting process is evaluated within the context of an application that involves cleaning/texturing severely corroded API 5L piping, which is commonly used for onshore/offshore petroleum transport applications. The results demonstrate that surface cleanliness and texture achieved via bristle blasting tools is on a par with grit blasting processes. That is, a near-white metal and white metal appearance of cleaned surfaces is routinely obtained, and is accompanied by an average peak-to-valley surface texture (R_z, microns) given by: $83 \geq R_z \geq 62$. Finally, careful study indicates that bristle blasting tools can remove corrosion at a rate in excess of one square meter per hour throughout the duration of tool life.

INTRODUCTION AND BACKGROUND

Steel structures play a vital role in supporting the infrastructure of transportation, habitat, and the distribution of goods and natural resources. In order to safeguard and maintain this infrastructure, polymer chemists have formulated advanced paints and coatings that can protect surfaces from corrosion and prolong the life/integrity of steel components. Nevertheless, these coatings are subject to environmental attack and eventually deteriorate, thereby requiring partial or complete removal prior to the reapplication of fresh coating. This cycle of repair/refurbishment is an important part of infrastructure maintenance programs that is both costly and time consuming. To this end, grit blasting has emerged as the principal method for surface cleaning and preparation chiefly because the process satisfies several important criteria, namely:
• Both the defunct coating and corrosion are simultaneously removed,
• Surfaces can be restored to meet the required visual cleanliness standards, and
• Coarse surface roughness profiles can be achieved that are deemed necessary prior to the application of protective paints and coatings.

Although grit blasting is the most widely used method for preparing steel surfaces, maintenance engineers are constantly searching for new/alternative surface treatment processes that can circumvent many of the difficulties and shortcomings that are associated with this

process. Most notably, for example, grit blasting is an expensive, cumbersome process that is neither environment nor user-friendly. The seriousness of health and safety issues has recently prompted the Environmental Protection Agency (USA) to propose national emission standards for controlling hazardous air pollutants associated with abrasive blasting [Kaelin and O'Malley (2008)]. At the same time, the Occupational Safety and Health Administration (USA) has recently issued directives that may have widespread implications on nearly all types of abrasive blasting processes/media [Kaelin and Liang (2008)]. Altogether, these concerns render the abrasive blasting process especially inefficient and poorly suited for applications involving local rehabilitation or "spot-repair", wherein steel surfaces are in need of immediate repair due to paint delamination and/or severe corrosion.

In this paper, a new process termed *bristle blasting* is introduced that utilizes a rotary power tool for simultaneously removing corrosion and generating an anchor profile. Although the bristle blasting tool has an appearance that resembles wire brush products, the underlying principles of operation are shown to have little, if any, commonality with brushing processes. Moreover, it is demonstrated in this paper that the bristle blasting process is very closely related to the impact mechanics behavior that is typically associated with grit blasting processes. Finally, the surface cleaning/profiling performance of bristle blasting tools is examined within the context of an application involving severely corroded API 5L steel piping, which is widely used in petroleum industries. The findings of this study show that the performance of bristle blasting tools can be likened to that of grit blasting operations. In addition, it is demonstrated that the performance and reliability of bristle blasting tools can be accurately forecasted over the duration of the tools service life.

REVIEW OF MEDIA/SURFACE INTERACTIONS

In this section, impact mechanics and surface interactions that are characteristic of grit blasting processes and brushing processes is reviewed. This review will help establish common ground for kinetic and kinematic comparison between the two different processes, and will also provide an historical background that relates grit blasting and the newly developed bristle blasting process.

a. Grit blasting process

Free-impact surface treatment processes involve the controlled use of projectile particles such as angular media (grit) or spherically shaped media (shot) of various size, composition, and hardness. When the former materials are used, the process is termed *grit blasting* or *abrasive blasting*, whereas use of the latter materials is termed *shot peening*. The process is depicted in Figure 1, whereby media having mass m_p undergoes free impact with
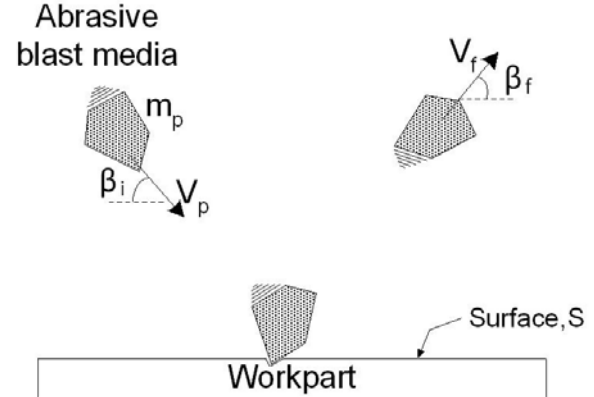

Figure 1: Pictorial representation of an abrasive blasting process with an arbitrary shaped grit.

target surface S. Process parameters include the media pre-impact speed v_p and arbitrary media entrance angle β_i, whereas the post-impact speed v_f and exit angle β_f of the media is a consequence of the elastic-plastic interaction that characterizes the impact event. On the basis of particle mechanics, the available kinetic energy e and working energy e_p of the media, respectively, is written

2

$$e = \tfrac{1}{2}\, m_p v_p^2 \; ; \tag{1}$$

$$e_p = \tfrac{1}{2}\, m_p v_p^2 \sin^2 \beta_i \tag{2}$$

where Eq. (2) presumes that the particle is unconstrained in the horizontal direction. As shown in Figure 1, the collision typically results in a pit or crater whose geometry is closely related to the shape of the propelled media. A significant volume of research has been reported on the crater geometry and the residual stress state induced in peened metallic surfaces. Although a review of these works is not undertaken in this paper, the reader can refer to pertinent examples of peening research that has been reported by Al-Obaid (1995) and Iida (1984). Less information, however, can be found in the literature concerning grit blasting processes. An earlier study reported on the subject by Jones and Gardos (1971) has examined the role that grit blast processing parameters play in the modification of stainless steel surfaces. Their work focused on examining the texture, dimensional change, and material removal performance of 100-mesh garnet used at a normal incident contact angle (β_i = 90°). A later investigation by Budinski and Chin (1983) examined the geometric nature of impact craters that are generated on various ductile metallic surfaces by single particle media comprised of 120 grit aluminum oxide. The authors were able to classify impact site features into the four basic categories shown in Figure 2,


Figure 2a: Pitting   Figure 2b: Plowing

Figure 2c: Shoveling   Figure 2d: Chipping
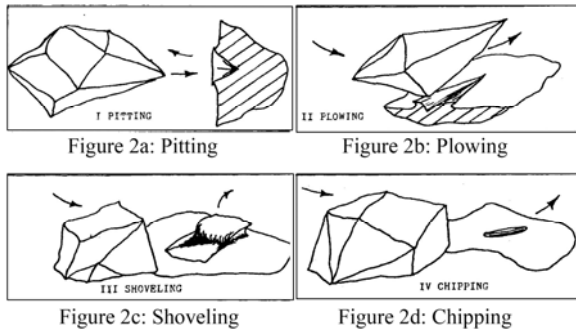
Figure 2: Basic types of the impact craters formed during an abrasive blasting process (figures taken from Budinski, and Chin, (1983)) featuring pitting (Fig. 2a), plowing (Fig.2b), shoveling (Fig.2c) and chipping (Fig.2d).

namely, pitting (Figure 2a), plowing (Figure 2b), shoveling (Figure 2c), and chipping (Figure 2d). Moreover, these impact features were found to be independent of both the composition and hardness of the substrate material. The author's conjectured that the evolution of texture and other features that characterize surface structure of grit blasting processes is a complex superposition of these fundamental impact signatures.

b. Wire brushing process

Wire brushing processes involve repetitive contact of bristle tips with a target surface. The process is shown in Figure 3, whereby bristles having length L, and mass m_b, are attached along the perimeter of a rotating hub having radius r_h and angular velocity ω. Here, the bristle/media is constrained at one end (namely, the *hub*) whereas the bristle tip is free to undergo periodic contact with the surface. On the basis
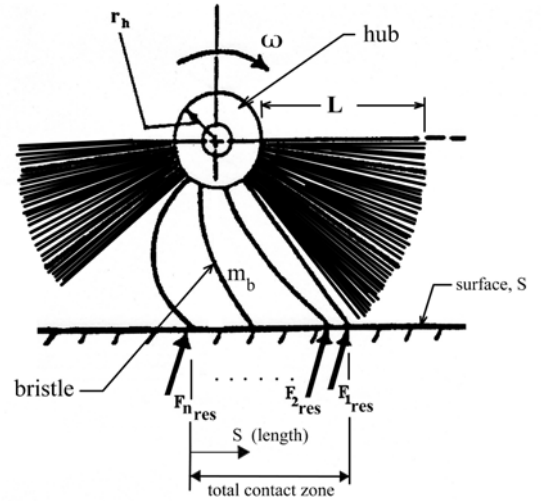

Figure 3: Planar view of wire brushing tool (lower portion only) illustrating bristle tips in contact with the workpart surface, S. The population of wires within the contact zone has been reduced to simplify the illustration of varying forces that each wire tip exerts on S as they transverse the contact surface.

of rigid body mechanics, the available kinetic energy of the rotating bristle is equivalent to the working energy of the bristle and can be written:

$$e_b = \tfrac{1}{2} m_b v_G^2 + \tfrac{1}{2} I_G \omega^2 \tag{3}$$

where e_b is the total kinetic energy of a bristle that undergoes orthogonal impact with surface S, v_G is the velocity of the mass center, and I_G is the mass moment of inertia of the bristle about mass center, G. Ordinarily, brush fabrication methods utilize fully populated, tightly packed bristles that exhibit considerable flexure during impact. Therefore, the collision/contact event between the bristle tips and the (relatively) rigid workpart surface is generally followed by an extended period of engagement along their mutual interface. Both the contact duration and the magnitude of the force exerted by the bristle tip onto the target surface are key issues that characterize the behavior and performance of bristle brushes. Although little information is available in the literature regarding the contact mechanics of brushing tools, Shia, et al. (1993,1998) have examined the theoretical dynamic contact forces exerted by a bristle tip onto a flat, rigid surface. Their work indicated that the contact event is characterized by an abrupt, large force that is subsequently followed by a retraction or *rebound* of the bristle tip from the rigid surface. As further investigation into the problem continued, an experimental method was developed by Stango, et al. (2005) and used for measuring the variation of bristle forces within the contact zone. In this work, the author's demonstrated that bristle tips do indeed
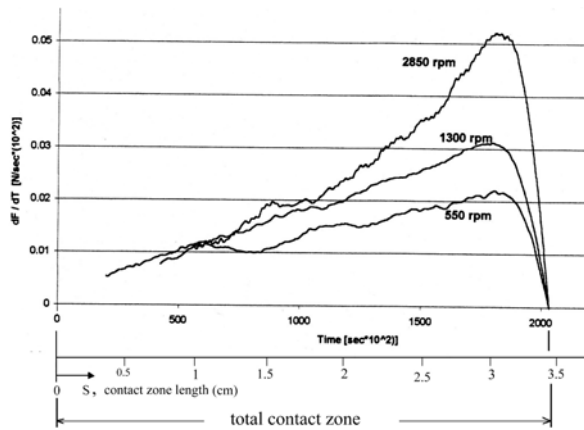
Figure 4: Experimentally measured average bristle force in contact zone for standard wire brush at three different spindle speeds (figure taken from Stango, et al., (2005)).

exert transient forces of significant magnitude near the point of entry within the contact zone.

A key outcome of this research is shown in Figure 4, where the measured average force exerted by bristle tips throughout the contact zone is shown for three different brush rotational speeds $n_1 = 550$ rpm, $n_2 = 1,300$ rpm, and $n_3 = 2,850$ rpm. In each case, the bristle forces within the initial portion of the contact zone rise abruptly as the speed is increased. However, one may observe that the bristle tips remain in contact with the surface throughout the entire excursion. Consequently, brushing processes are known to generate *score markings* or *striations* along the entire region of contact.
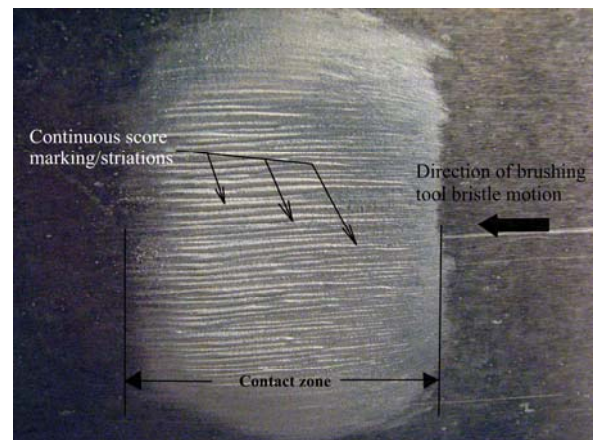
Figure 5: Score markings or striations associated with a typical wire brushing process.

These markings are easily identified in Figure 5, and have been the subject of considerable investigation in the literature by Stango, et al. (1991), Cariapa, et al., (1991), Stango, et al. (1995), and Overholser, et al. (2003).

As an outcome of the research completed by Stango, et al. (2005), the author's concluded that with proper bristle design, rotary bristle tools could be reconfigured to perform impact processes such as peening operations. This concept was further explored with the aid of a high-speed digital camera by Wojnar (2006) and has shown that *single-crater* indentation can be regularly obtained by bristle tips, pending properly designed bristle geometry. That is, impact of the bristle tip with a targeted surface is immediately followed by retraction or *rebound* of the tip, thereby resulting in the formation of a crater that is similar to blasting and peening processes. This finding provides a cornerstone

4

for altering the behavior of bristle dynamics as well as the morphology of surfaces that can be generated by rotary bristle tools, and is further discussed in the next section.

BRISTLE BLASTING TOOL SURFACE INTERACTIONS

a. Monofilament impact

To begin, the dynamic response of a single bristle or *monofilament* is examined using high speed digital video camera. The geometry of three differently configured bristles whose dynamic response will be examined are shown in Figure 6, and consists of steel wire having reverse-bent knee (Figure 6a), without bend

| (a) | (b) | (c) |
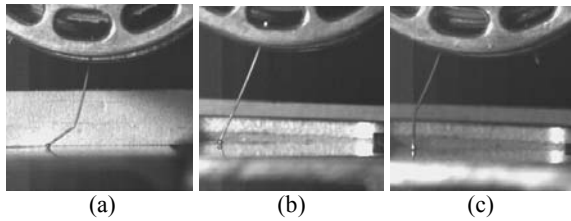
Figure 6: Geometry of three differently configured bristles featuring 6a (reverse bent knee). 6b (straight without bend) and 6c (forward bent knee).

(Figure 6b), and forward-bent knee (Figure 6c). In each case, bristles having overall length L = 2.9 cm, diameter d = 1 mm, are attached to a hub having radius r_h = 2.9 cm which rotates at constant speed n = 2,800 rpm. The target surface
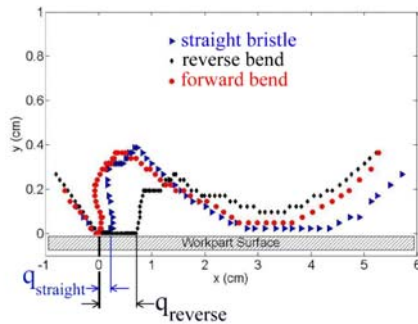
Figure 7: Kinematic response of the three different types of bristles shown in Fig.5

is composed of flat steel that has been hardened and ground. Thus, the kinematic response of the

bristle tip that ensues immediately following impact is shown in Figure 7 for each basic filament shape. Although bristle tip impact/retraction is exhibited by all three filaments, one may observe that *sliding contact* occurs between the bristle tip and target surface for only two bristle configurations, namely the reverse-bent knee (diamond) and straight bristle (triangle). However, the forward bent bristle (circle) undergoes impact and immediately rebounds from the target surface. This impact/rebound phenomenon is not a tool signature associated with brushing processes. Therefore, it is conjectured that rotary tools fabricated from forward-bent bristles will generate a *crater* or *micro-indentation*, which is uncharacteristic of brushing tools.

The actual crater that is generated at the tip/surface interface for forward bent bristles (Stango and Khullar, (2008)) is shown in Figure 8 for API-5L steel. This crater has been
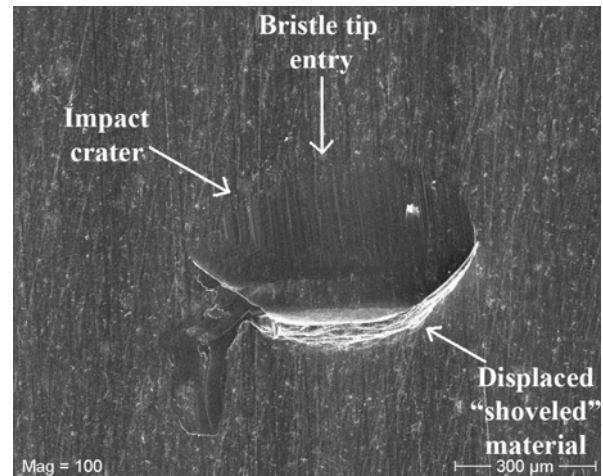
Figure 8: SEM Image of micro-indentation caused by forward bent bristle tip impact with flat, ground API 5L surface.

generated by a sharp, hardened bristle tip that is similar to those depicted in Figure 9. A direct comparison of this micro-indentation with those reported by Budinski and Chin (1983) (see Figure 2) indicates that the signature of bristle tip impact is similar to that generated by grit blast shoveling deformation shown in Figure 2c. It is surmised, therefore, that repetitious contact of bristle tips with a ductile surface will yield textures that are consistent with characteristic

features of grit blasting processes. This supposition is further examined in the next section.

b. Bristle blasting tool: surface morphology and cleanliness

In Figure 9 the composition and construction of a typical bristle blasting tool is shown. The
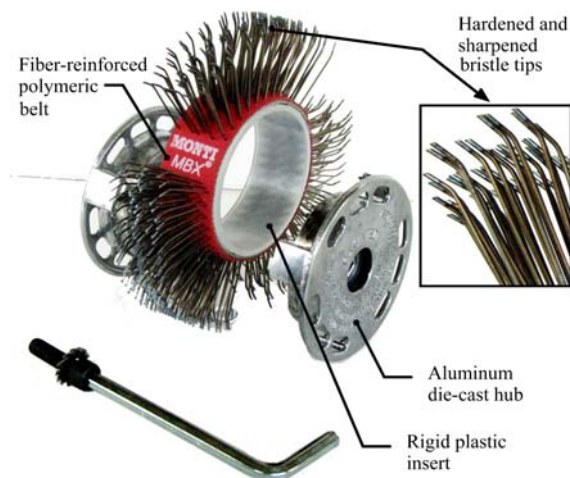
Figure 9: Design and construction of the bristle blasting tool. Upon assembly of components shown, tool is ready to be mounted on spindle

tool consists of steel wires that are bent forward and protrude through a fiber-reinforced polymeric belt that is fitted over a rigid plastic support ring. Subsequently, an interlocking die-cast hub secures the assembly to the power tool spindle shown in Figure 10, which operates at approximately 2,500 rpm. The hand-held power
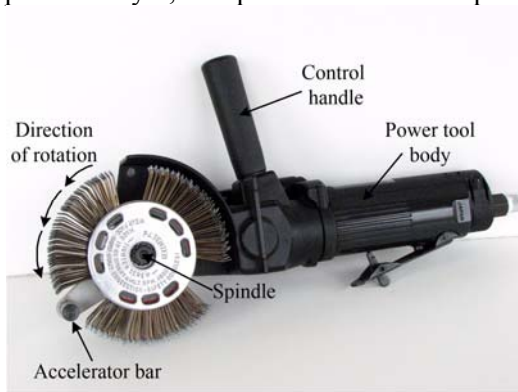
Figure 10: Bristle blasting tool mounted on the power tool spindle. Bristle blasting system shown is ready to be used.

tool is then used to clean and profile the severely corroded API 5L pipe specimen appearing in Figure 11. A cursory evaluation of the initial

Figure 11: Section of 6 in. diameter API 5L piping used for evaluating corrosion removal performance of bristle blasting tool

surface condition suggests that *SSPC Condition D* (100% rust with pits) characterizes the severity of the internal and external corroded surfaces.

In Figure 12 the corrosion-free surface is shown after bristle blasting an interior section of the vessel wall. For comparison purposes, the initial condition of the corroded interior surface
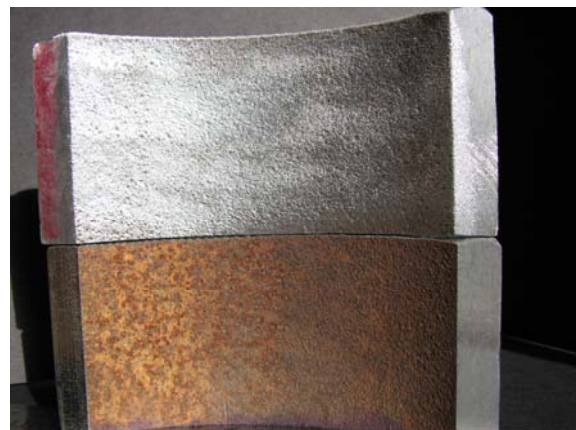
Figure 12: Interior of API 5L piping in as-received condition (bottom) and after bristle blast cleaning (top).

has been place directly below the cleaned coupon. One may observe that the cleaned surface has a uniform appearance and is free of any residual corrosion. In order to further

examine the degree of cleanliness and the morphology of surfaces generated by the bristle blasting process, scanning electron micrographs of the treated surface are shown in Figures 13a and 13b. Careful examination of Figure 13a (20x) indicates that no corrosive pits remain, and

<div align="center">(a)   (b)</div>
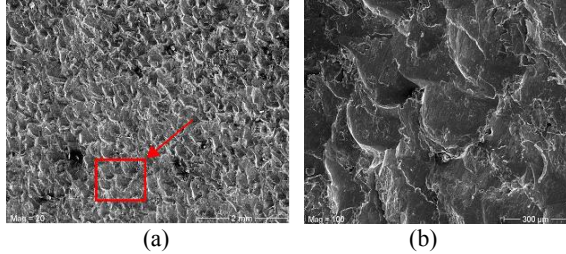
Figure 13: Scanning electron micrographs of the bristle blast treated surface shown in Fig.11). Fig.(13a) at 20x, and Fig. (13b) at 100X of the region indicated by the arrow.

that the treated surface has a uniform/repeated pattern consisting of micro–indentations. Each micro-indentation is evidently associated with the impact/rebound of bristle tips, and bears a strong semblance to the impact crater shown in Figure 8. Higher magnification (100x) of the region outlined in Figure 13a is shown in Figure 13b, and clearly indicates craters that were individually formed by bristle tip impact during the cleaning process.

Several observations can now be made regarding the degree of cleaning offered by the bristle blasting tool in relation to other standard methods that are commonly used in a production environment. A direct comparison of surfaces prepared by bristle blasting with photographs that are published by the Steel Structures Painting Council (SSPC-VIS 3) for various power tools and hand tools indicates that the current approach clearly outperforms conventional *wire brushes*, *sanding disks, rotary flap and needle gun* processes. Likewise, a comparison of bristle blast cleaning performance can be made with SSPC photographs that are published for dry abrasive blast cleaning processes (SSPC-VIS 1). In this case, thoroughness of the bristle blasting process apparently exceeds the cleanliness that is achieved by *brush-off blast cleaning* (SP 7), *industrial blast cleaning* (SP 14*)*, and *commercial blast cleaning* (SP 6). The result obtained by bristle blast cleaning, however, does

appear to be comparable to *near-white blast cleaning* (SP 10) and *white metal blast cleaning* (SP 5).

KINETIC ENERGY CONSIDERATIONS

Grit/Bristle Kinetic Energy Equivalence

On the basis of Eq. (2) and Eq. (3), the configuration and operating conditions of bristle blasting tools can be developed that generate an *equivalent kinetic energy* to grit blasting processes. In this section, two different approaches are examined for generating bristle motion and therefore, the content of bristle kinetic energy. The first approach is based upon computing the kinetic energy of a bristle under standard operating conditions, that is, the bristle is attached to a hub which rotates at constant speed. The second approach examines the bristle kinetic energy that is generated due to a disturbance that is strategically introduced into the oncoming path of the bristle tip just prior to contact with the target surface. For illustration, examples are given for each approach using a wire bristle having dimensions L = 2.7 cm, d = 0.73 mm, forward bend angle 38 degrees, with hub radius r_h = 2.75 cm. The kinetic energy equivalence between the aforementioned bristle and grit blast media will be based upon the use of steel grit in conjunction with the commonly specified nozzle entrance angle α (formerly $β_i$) = 70 deg.
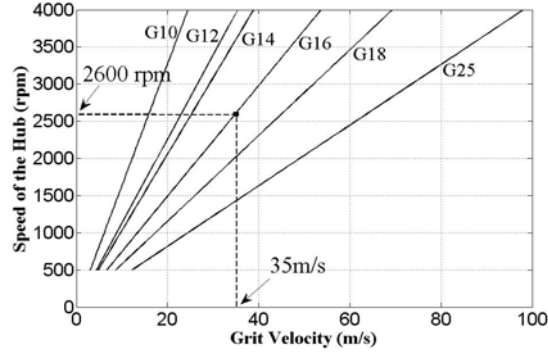
a. Case 1: Standard bristle motion

Kinetic energy equivalence for the two different processes is obtained by the direct use of Eq. (2) and Eq. (3). Thus, the equality of media energies yields:

$$n = \frac{30 v_p}{\pi} \left[\sqrt{\frac{m_b}{m_p} \frac{\frac{1}{12}L^2 + (\frac{L}{2}+r)^2}{\sin^2 \alpha}} \right]^{-1} \quad (4)$$

where n(rpm) = 30 ω/π is the spindle speed of the bristle blasting tool, and bristle length L is assumed to be the same for both straight and

forward-bent bristles. On the basis of the previously cited bristle dimensions, the relationship between spindle speed and grit velocity is shown in Figure 14 for several different steel media having the measured mass


Figure 14: Relationship between spindle speed and grit velocity for several different steel media for the case of standard bristle motion. (Note: spindle speed 2600 rpm corresponds to grit velocity of 35 m/s for G16)

ratios m_b/m_p. Thus, the use of G16 media (diameter $\approx$ 1mm) corresponds to the approximate spindle speed n = 2,600 rpm with a grit velocity of 43 m/s.

b. Case 2: Enhanced bristle motion

As an alternative to standard bristle motion, this approach explores the feasibility of increasing the bristle velocity v_b by placing an obstruction in the path of bristle tips just prior to their contact with the target surface. In practice, the obstruction or *accelerator bar*, (refer to Figure 10) is rigidly attached to the frame of the power tool. As shown in Figure 15, pre-contact of the bristle tip with the accelerator bar at point
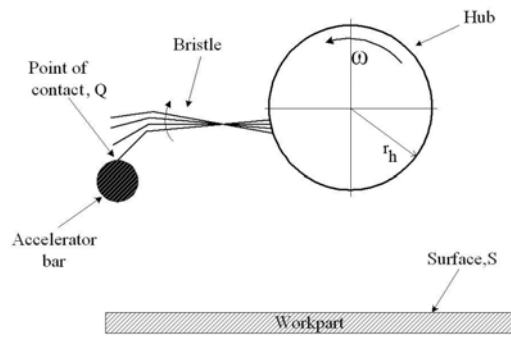
Figure 15: Retraction of the bristle tip on contact with the accelerator bar

Q causes impact and subsequent retraction of the bristle tip, thereby providing storage and release of additional energy as the bristle accelerates toward the target surface. This concept is further illustrated in Figure 16, where the anticipated bristle tip motion is shown after contact has been made with point Q. One may
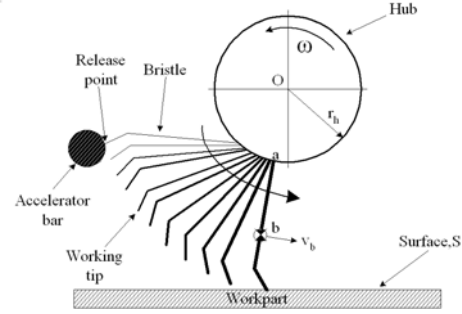
Figure 16: Acceleration of the bristle tip towards the target surface upon release from the accelerator bar.

observe that the impending motion of the bristle can be computed by superimposing the rotational speed with the supplemental speed associated with the natural frequency of the bristle. In practice, the natural frequency of the bristle can be ascertained by experimental observation in conjunction with elementary dynamic analysis of the system. Thus, with reference to the mass center of the bristle, the enhanced velocity is written:

$$v_b = v_a + v_{b/a} \qquad (5)$$

where v_b ($\equiv v_G$) is the velocity of the bristle mass center, v_a is the velocity on the hub perimeter, and $v_{b/a}$ is the relative velocity, namely,

$$v_{b/a} = \frac{L}{2}\omega_b(t) \qquad , \qquad (6)$$

where $\omega_b(t)$ is the time-dependent angular velocity of the bristle mass center as energy is released during forward excursion of the bristle. Based upon elementary mechanics (see, for example, Thompson (1965)), the impending rigid body bristle motion can be modeled by a simple mechanical system whose governing equation is:

8

$$\ddot{\theta} + \omega_n^2 \theta = 0 \qquad (7)$$

where the standard over-dot notation (¨) has been introduced to indicate the (second order) time derivative, ω_n is the natural frequency of the freely oscillating bristle, and θ is the time-dependent angular displacement of the bristle measured from the point at which the tip is released from the accelerator bar to the equilibrium (i.e., unloaded) configuration.

Equation (7) is a standard linear homogeneous ordinary differential equation whose solution is given by

$$\theta = C_1 \cos \omega_n t + C_2 \sin \omega_n t \qquad (8)$$

$$\dot{\theta} = -C_1 \omega_n \sin \omega_n t + C_2 \omega_n \cos \omega_n t \qquad (9)$$

where C_1, C_2 are constants to be determined, and

$$\omega_b = \dot{\theta} = d\theta/dt. \qquad (10)$$

Thus, careful examination of high speed video yields the following bristle natural frequency and initial conditions, respectively:

$$\omega_n = 1338 \ rad/s \qquad (11a)$$

$$\theta(0) = 0.9032 \ rad \qquad (11b)$$

$$\dot{\theta}(0) = 0 \qquad (11c)$$

Substituting Eqs. (11) into Eqs. (8) and (9) one obtains $C_1 = 0.9032$ and $C_2 = 0$; therefore,

$$\theta(t) = 0.9032 \cos \omega_n t \qquad (12)$$

$$\dot{\theta}(t) = \left| 0.9032 \ \omega_n \sin \omega_n t \right| \qquad (13)$$

Specifically, Eq. (13) is maximum at the angular position $(\omega_n t) = \dfrac{\pi}{2}$, which corresponds to $\theta = 0$, i.e., the bristle equilibrium (unloaded) configuration. The use of Eq. (10) in conjunction with Eq. (13) facilitates the computation of the bristle mass center velocity

appearing in Eq. (5). This, in turn, results in the *enhanced* bristle kinetic energy e_b* as follows:

$$e_b^* = e_T^* + e_R^* \qquad (14)$$

where e_T^* is the translational kinetic energy, e_R^* is the rotational kinetic energy, and

$$e_T^* = \frac{1}{2} m_b \left(\left\{ \frac{L}{2} K \right\} + \frac{\pi}{30} n \, r_h \right)^2 \qquad (15)$$

$$e_R^* = \frac{1}{2} \left(\frac{m_b L^2}{12} \right) (K)^2 \qquad (16)$$

where $K = 0.9032 \, \omega_n \sin \omega_n t$, n is the arbitrary (but constant) spindle speed, and $\omega_n t = \pi/2$ (for maximum kinetic energy) as previously discussed.

Potential benefits of the enhanced bristle kinetic energy can now be evaluated by equating the grit kinetic energy (Eq. (2)) and enhanced bristle kinetic energy (Eq. (14)) to obtain the following:

$$v_p = \frac{1}{\sin \alpha} \sqrt{\frac{m_b}{m_p} \{A_1 + A_2\}} \qquad (17)$$

where

$$A_1 = \left(\frac{L}{2} K + \frac{\pi}{30} n_R r_h \right)^2 \qquad (18)$$

$$A_2 = \frac{1}{12} (L \, K)^2 \qquad (19)$$

For comparison with the results reported in Figure 14, the relationship between spindle speed and grit velocity is re-examined in Figure 17 for several different steel media having the measured mass ratios m_b/m_p. Thus, direct comparison of G16 media with motion enhanced bristle tools having the spindle speed n = 2,600 rpm yields a corresponding grit velocity of 79 m/s. When compared with the previously computed grit speed for standard bristle motion

(i.e., 35 m/s), the current equivalent grit speed is enhanced by 125%.
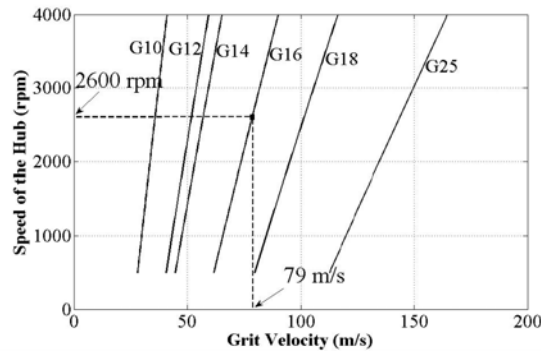
Figure 17: Relationship between spindle speed and grit velocity for several different steel media for the case of enhanced bristle motion. (Note: spindle speed 2600 rpm corresponds to grit velocity of 73 m/s for G16)

MATERIAL REMOVAL AND TEXTURE PERFORMANCE OF BRISTLE BLASTING PROCESS

In this section, a case study is presented that examines the material removal performance of bristle blasting processes that utilize enhanced bristle motion. As one may expect, the configuration/sharpness of bristle tips can play an important role in forming the crater/micro-indentation that appears in Figure 8. Thus, the initial chisel-shape of bristle tips appearing in Figure 9 is subject to eventual wear during the corrosion removal process which, in turn, reduces the capacity of the bristle tip to penetrate the surface. In order to examine both the material removal performance and the role that progressive wire tip-wear plays in bristle blasting processes, considerable experimentation has been carried out, and a portion of these results are shown in Figure 18 and Figure 19.

In Figure 18, the material removed (gram weight) from a flat API 5L specimen is measured and reported by using bristle blasting tools that have acquired various periods of operation/in-service use. Thus, the material removed by tools having 3 different "ages", namely, 5 min. (triangle), 25 min. (square), and 72 min. (diamond) of service life are reported.

The material removal process was carried out by inserting/penetrating the rotating tool into the specimen to a nominal depth of 4 mm, and
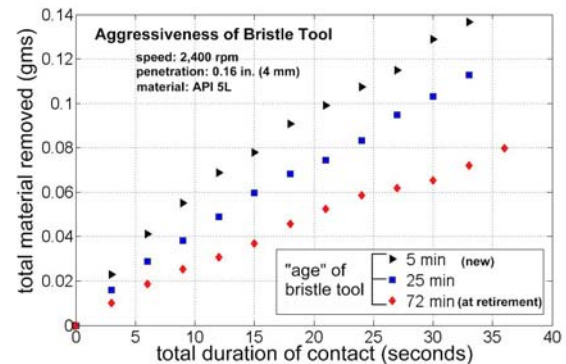
Figure 18: Measured material removal rate for API 5L flat specimen, using bristle tools having various periods of service. Approximate bristle tool specifications: face width: 22 mm, hub radius: 27.5 mm, bristle wire diameter: 0.73 mm, bristle length: 27 mm, total bristle population ~480.

allowing the tool to extract parent material from the specimen for several prescribed time intervals without interruption. At the conclusion of each interval, the specimen was weighed using a high-resolution electronic balance, and
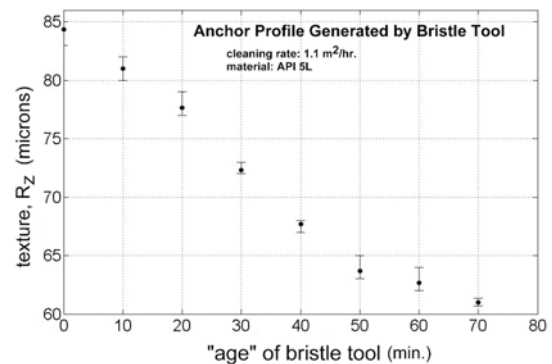
Figure 19:. Variation of surface texture/anchor profile as bristle tool progressively ages. Approximate bristle tool specifications: face width: 22 mm, hub radius: 27.5 mm, bristle wire diameter: 0.73 mm, bristle length: 27 mm, total bristle population ~480.

the differential material removed was recorded. The results indicate that the material removal capacity of the tool regularly decreases as its duration of use increases. Nevertheless, the tool

retains the ability to remove material from the specimen even up to the time at which tool retirement is recommended (i.e., ~ 70 min.).

As the tool progressively ages, one may expect that the texture/anchor profile performance of the tool will likewise be affected. Therefore, the relationship between surface texture (R_Z, microns) and tool age (minutes of service) has been examined and is reported in Figure 19. The results reported in Figure 19 are the averaged value of 3 separately recorded texture measurements that were obtained using standard press-film replica tape. This result indicates that the new (i.e., as received) tool generates an anchor profile of R_Z ~ 84. However, with increased use, the anchor profile performance of the tool progressively declines to R_Z ~ 62 at the conclusion of the tools life.

SUMMARY AND CONCLUSION

Kinematic Comparison Among Grit Blast, Wire Brush, and Bristle Blast Surfaces

Bristle geometry plays a key role in the dynamic response and impact signature that is characteristic of rotary bristle tools. Rotary tools that are comprised of forward-bent bristles can exhibit impact and immediate retraction from the target surface, thereby generating a crater or micro-indentation that neither replicates brushing tool behavior, nor generate surfaces that are characteristic of brushing processes. The contact mechanics and surfaces generated by tools that exhibit this behavior is, however, closely related to both grit and/or shot blasting processes. It is proposed, therefore, that impact tools of this variety be appropriately termed *bristle blasting tools*, and their implementation in surface treatment operations be termed *bristle blasting processes*.

Kinetic Energy Considerations

Kinetic energy can provide a rational basis for establishing dynamic equivalence between grit blast media and bristle blasting tools. Significantly enhanced kinetic energy of bristles can be obtained by strategically placing an obstruction or *accelerator bar* into the oncoming path of rotating bristles.

Corrosion Removal Performance

Comparison among SSPC Visual Standards for power hand tools, dry abrasive blast cleaning, and surfaces generated by bristle blasting tools suggests that the bristle blasting process can generate surfaces whose cleanliness outperforms various existing power tools and hand tools, as well as several dry abrasive blast cleaning processes. The cleanliness of bristle blast surfaces closely corresponds to near-white metal (SP 10) and white metal (SP 5). In addition, the material removal and anchor profile performance of bristle blasting tools can be accurately forecasted over the duration of tool life (approximately 1 hour).

REFERENCES

Al-Obaid. Y.E., 1995, Shot Peening Mechanics: Experimental and Theoretical Analysis. Mechanics of Materials, 19, 251-260.

Budinski, K. G., and Chin, H, 1983, Surface Alteration in Abrasive Blasting, Wear of Materials, 311-318.

Cariapa, V., Stango, R.J., Liang, S.K., and Prasad, A., 1991, Measurement and Analysis of Brushing Tool Performance Characteristics: Part 2: Contact Zone Geometry, ASME Journal of Engineering for Industry, 113, 290-296.

Iida, K., 1984, Dent and Affected Layer Produced By Shot Peening, Proceedings, 2nd International Conference on Shot Peening, Chicago, USA, 217-227.

Jones, J. R., and Gardos, J.M., 1971, An Investigation of Abrasive Blasting, Journal of ASLE, 6, 393-399.

Kaelin, A., and Liang, S., 2008, New OSHA Program Targets Silica, Other Blast Cleaning Hazards, Journal of Protective Coatings and Linings, 25 (6), 47-51.

Kaelin, A., and O'Malley, D., 2008, What's New with Regs for Surface Prep?, Journal of Protective Coatings and Linings, 25 (6), 41-45.

Overholser, R., Stango, R.J., and Fournelle, R.A., 2003, Morphology of Metal Surface Generated by Nylon/Abrasive Brush, Journal of Machine Tools and Manufacture, 43, 193-202.

Shia, C. Y., Stango, R.J., and Heinrich, S.M., 1993, Analysis of Contact Mechanics for Circular Filamentary Brush/Workpart System- Part I: Modeling and Formulation and, Part II: Solution Method and Numerical Studies, Proceedings of the ASME Symposium on Contact Problems and Surface Interactions in Manufacturing and Tribological Systems,67 (4), 171-190.

Shia, C. Y., Stango, R.J., and Heinrich, S.M., 1998, Analysis of Contact Mechanics for Circular Filamentary Brush/Workpart System, ASME Journal of Manufacturing Science and Engineering, 120, 715-721.

SSPC-VIS 1, Guide and Reference Photographs for Steel Surfaces Prepared by Dry Abrasive Blast Cleaning, Steel Structures Painting Council, Pittsburgh, PA 15213-3724.

SSPC-VIS 3, Visual Standard for Power- and Hand-Cleaned Steel, Steel Structures Painting Council, Pittsburgh, PA 15213-3724.

Stango, R. J., and Khullar, P., (accepted, June, 2008) ACA Journal of Corrosion and Materials.

Stango, R. J., Cariapa, V., and Zuzanski, M., 2005, Contact Zone Force Profile and Machining Performance of Filamentary Brush, ASME Journal of Manufacturing Science and Engineering, 127, 217-226.

Stango, R.J., Cariapa, V., Prasad, A., and Liang, S.K., 1991, Measurement and Analysis of Brushing Tool Performance Characteristics: Part 1: Stiffness Response, ASME Journal of Engineering for Industry, 113, 283-289.

Stango, R.J., Fournelle, R.A., and Chada. S., 1995, Morphology of Surfaces Generated by Circular Wire Brush, ASME Journal of Engineering for Industry, 117, 9-15.

Thompson, W.P., 1965, Vibration Theory and Applications, Prentice-Hall, Inc., Englewood Cliffs, NJ, USA.

Wojnar, N., 2006, Design and Application of Rotary Bristle Brush for Peening Applications, M.S. Thesis, Marquette University, Milwaukee, WI 53233.